AIAA 2007-1003

Power Transmission to a Micro Aerial Vehicle

Shuhei Komatsu,[1] Kenta Katsunaga,[2] Ryoji Ozawa,[3] Kimiya Komurasaki,[4] and Yoshihiro Arakawa[5]
The University of Tokyo, Kashiwa, Chiba 277-8561, Japan,

A microwave power feed system to a Micro Aerial Vehicle is under development using a 5.8GHz beam irradiated by a phased array antenna. Transmission power is 3.5W and the beam divergence angle is 9deg. The beam is steerable in the range of –9 deg to 9 deg in the *x* and *y* directions. The vehicle tracking system is realized using a 2.45GHz microwave pilot signal and the software retro-directive function. A polarity-free patch antenna is proposed as a receiver antenna for constant power supply to a circling vehicle. Its polarity-free characteristics are measured and the antenna shape is optimized.

Nomenclature

d	=	array pitch
D	=	array antenna diameter
E	=	amplitude of the microwave electric field
h	=	altitude
V	=	detector output
x, y	=	coordinates
α	=	incident angle of the pilot signal to the antenna
δ, φ	=	phase difference
ψ	=	angle of wave polarization to antenna resonance direction
λ	=	wavelength
θ_{str}	=	steering angle

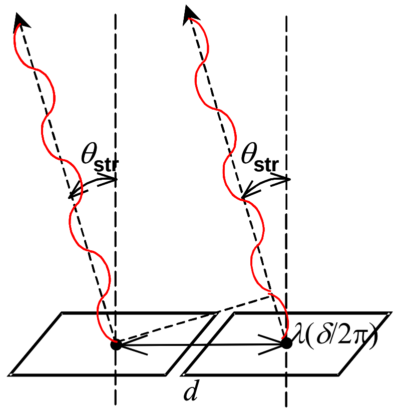

Figure 1. The concept of beam steering by a phased array antenna.

I. Introduction

At the University of Tokyo, “Innovative Aerial Robot Project” focusing on Unmanned / Micro Aerial Vehicles is being carried out as a part of the Japanese 21st century COE program. Microwave power transmission to a Micro Aerial Vehicle has been studied in this project. Electrical power for MAV’s propulsion system is provided remotely from the ground power station.

The microwave phased array technology has been intensively developed for power transmission from a Space Solar Power Station to the ground.[1,2] This technology was applied to this project in this study. Pointing of the microwave beam was achieved by controlling the phase of element microwaves of the antenna array, not by mechanical control of the antenna’s attitude. The principle of beam steering by a phased array antenna is schematically shown in Fig. 1. The steering angle θ_{str} is a function of the phase difference δ between the neighboring elements as $d\sin\theta_{str}=\lambda\delta/2\pi$.

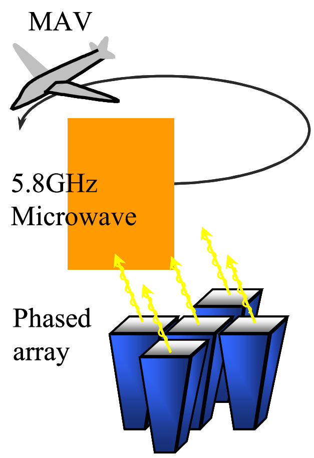

Figure 2. Schematic of microwave energy transmission to a MAV by a phased array.

Figure 2 shows the concept of microwave power transmission to a MAV by a phased array antenna. Power is transmitted while a MAV is

[1] Graduate student, Department of Advanced Energy, Kashiwanoha 5-1-5, Kashiwa
[2] Graduate student, Department of Advanced Energy, Kashiwanoha 5-1-5, Kashiwa
[3] Graduate student, Department of Aeronautics and Astronautics, Hongo 7-3-1, Bunkyo, Tokyo
[4] Associate professor, Department of Advanced Energy, Kashiwanoha 5-1-5, Kashiwa, Chiba, Senior member
[5] Professor, Department of Aeronautics and Astronautics, Hongo 7-3-1, Bunkyo, Tokyo, Senior member

circling above the antenna. In our previous researches,[3,4] a five-element phased array antenna as shown in Fig. 3 was developed. Table 1 shows its specifications.

Table 1. Specifications of the five-element phased array antenna

Parameters	values
microwave frequency	5.8GHz
wavelength, λ	51.7mm
total transmission power, P	3.5W
array pitch, d	110mm (d/λ=2)
diameter of the array, D	330 mm

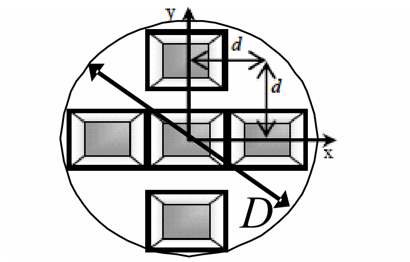

Figure 3. Geometry of the five antenna elements of the array.

Microwave of 5.8 GHz is provided by a Field Effect Transistor oscillator and divided into five elements as illustrated in Fig. 4. The phase of element microwave can be controlled individually using four 6-bit phase shifters, whose phase resolution is 5.6 deg. (The middle antenna has a locked phase.). Five FET amplifiers with the output power of 0.7W each are used to have totally 3.5W output power. Each microwave is guided to an antenna through a coaxial cable. Horn antennas, whose exit plane size is Δx=110mm and Δy=81mm, are used as element transmitters. The beam is linearly polarized in the y-direction.

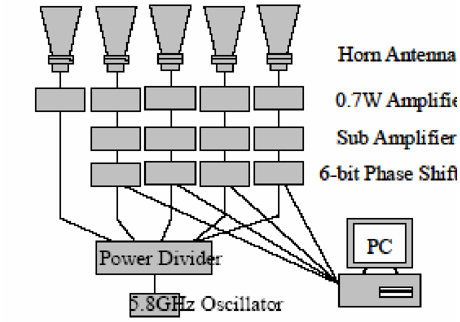

Figure 4. Array antenna system

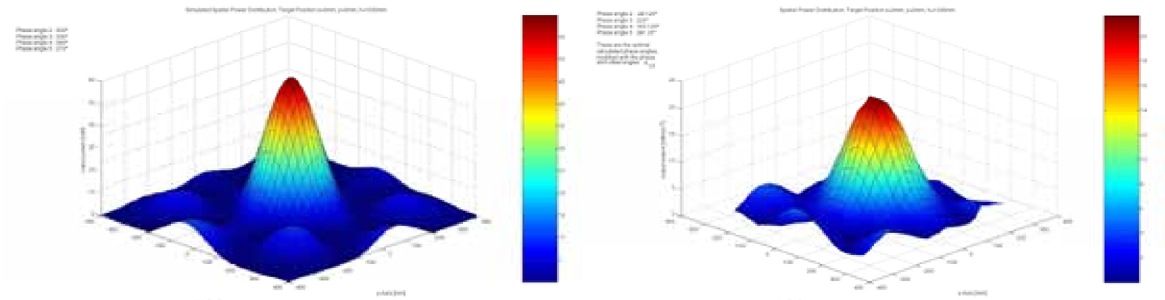
(a) Computed

(b) Measured

Figure 5. E_y distribution at h=1m

Figure 5 shows the computed and measure beam profiles. Measured main-lobe fractional energy and main-lobe beam divergence angle are well agreed with the calculated ones. Figure 6 shows the computed properties as a function of θ_{str}. The beam divergence was constant at about 9 deg, which corresponds to the beam quality of M^2=1.6.

Tracking of a flying vehicle would be challenging. Software retro-directive function will help its quick and precise tracking. The objectives of this study are the auto tracking of a moving object and the polarity free microwave rectification. Those two are inevitable technologies for power transmission to a MAV

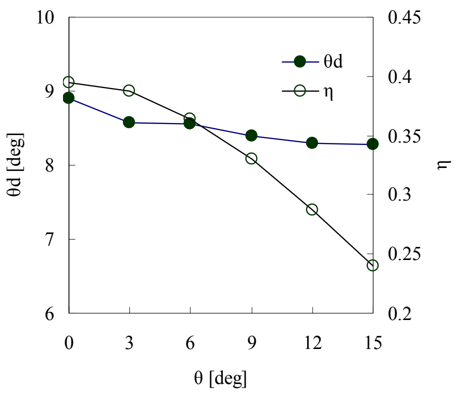

Figure 6. Computed main-lobe fractional energy and beam divergence angle.

II. Auto Tracking System

Figure 7 shows the tracking system: a pilot signal transmitter, receiver antennas, and a PC. Firstly, a flying vehicle sends a pilot signal toward two pairs of receiver antennas: one is for the *x* direction and another is for the *y* direction. Secondly, the incident angles α_x and α_y of the pilot signal to the antennas are estimated from the phase differences between neighboring antennas in each direction by a PC software. Finally, the phase shifters of the phased array system are controlled according to the estimated α_x and α_y via the digital output of the PC, and a microwave beam is pointed toward the vehicle. This system is called a software retro-directive function system.

Figure 8 shows the block diagram of the tracking antennas and microwave signal operation system. A pair of patch antennas is aligned with the pitch of λ. The phase difference of π/2 is added to one of the antenna lines as indicated in the figure. Dividing each of these waves into two, both waves are combined using a coupler.

A flying target is far enough to model the incident wave as a plane wave. When the incident angle to the antennas is α, the phase difference φ appears between the antennas as

$$\varphi = 2\pi \sin\alpha \quad . \tag{1}$$

Then amplitude of the combined electric field E_{com} can be expressed as a function of φ as,

$$E_{com}^2 = \left[E_0 \sin\left(\omega t + \pi/2\right) + E_1 \sin\left(\omega t + \varphi\right)\right]^2 . \tag{2}$$

In the ideal condition, E_0 is identical to E_1. Then, Eq.(2) is simplified as

$$E_{com}/E_0 = \sqrt{2 + 2\cos\left(\pi/2 - \varphi\right)} . \tag{3}$$

The combined wave is rectified using a microwave detector: the amplitude is indicated as V_{com}. The divided waves are also monitored as V_0 and V_1. These voltages are transmitted to the PC via an analog input module. Because the detector output V is almost proportional to E^2, then Eq.(2) is expressed as

$$V_{com}/V_1 = 2 + 2\cos\left(\pi/2 - \varphi\right) \tag{4}$$

As plotted in Fig. 9, α can be uniquely determined from the measured V_{com}/V_1. The detectable range of α is –13 deg to +13 deg, that is enough for tracking a vehicle because the steerable angle θ_{str} of the phased array is – 9deg to +9 deg.

To verify this software tracking method, the microwave signal operation system was simulated using a oscillator and a phase shifter instead of antennas as indicated in Fig. 10. Figure 11 shows the result. Power loss at the phase shifter has been compensated. The result shows that α can be uniquely determined from V_{com}.

All the units have not been integrated yet. We'll demonstrate the auto-tracking and pointing performance using a MAV model in near future.

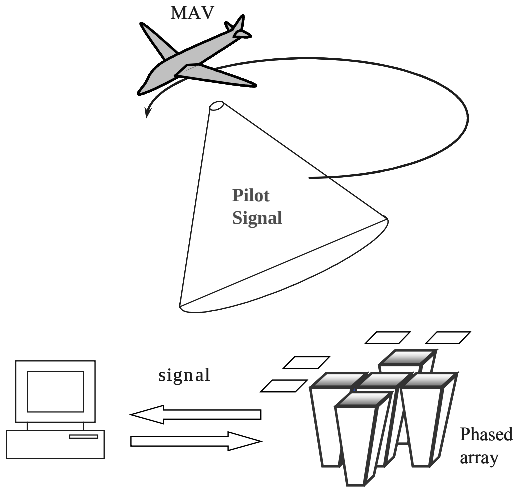

Figure 7. Tracking system

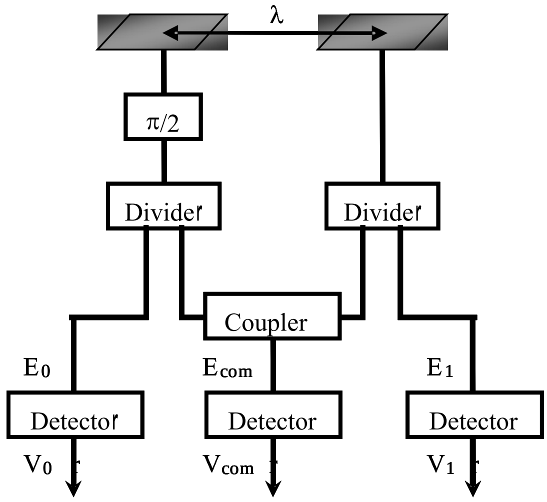

Figure 8. The block diagram of the tracking antennas and microwave signal operation system.

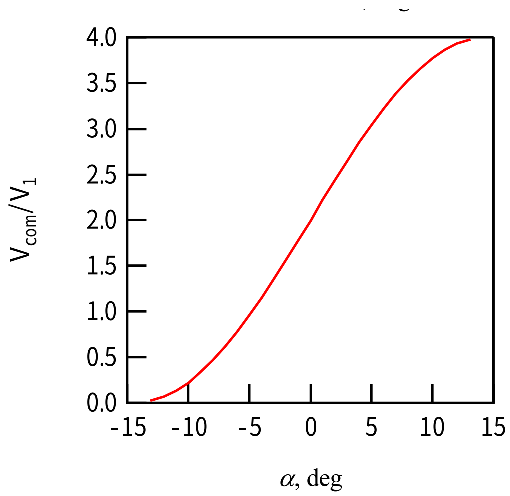

Figure 9. Expected relationship between incident angle α and output signal V_{com}/V_1.

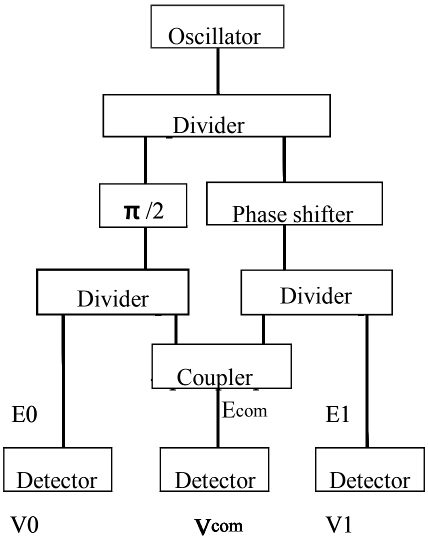

Figure 10. Block diagram for experimental simulation of the software retro-directive system.

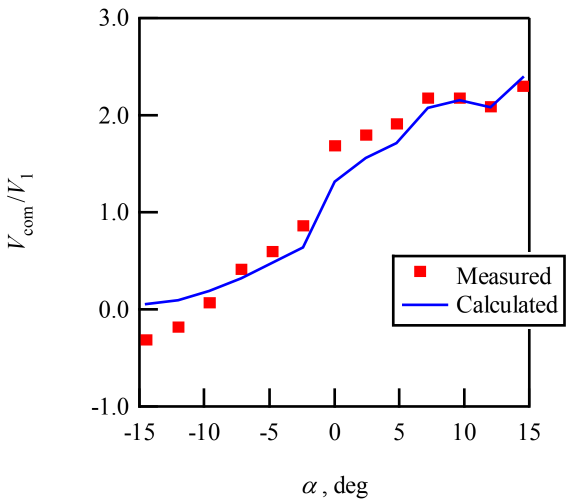

Figure 11. Simulated result.

III. Polarity Free Rectenna

A rectenna array will be installed on a MAV. The MAV's yaw angle changes while circling. When the transmitted microwave is linearly polarized, the receivable power will change with the angle ψ between the wave polarization and the antenna resonance direction on a MAV. For constant power supply, we studied a polarity-free rectenna system.

Generally, there are two methods to make receiver antennas polarity-free: One method is a Unit of Multiple Dipole antennas (UMD) with different polarization angles as shown in Fig 12 (a). Another method is a Polarity-Free Patch antenna (PFP) which smoothes the polarization angle dependency using one antenna element.

Because the UMD antenna is composed of the existing dipole antennas, the polarity angle's dependency and the power conversion efficiency are predictable. Furthermore, a flexible UMD sheet has been developed. However, larger receiving area is necessary to achieve polarity-free antenna arrangement than a single-polarity dipole antenna array, resulting in lower efficiency.

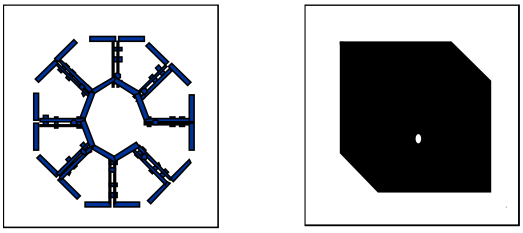

(a) Unit of Multiple Dipoles (b) A Polarity-Free Patch

Figure 12. Polarity-free receiver antennas

The PFP antenna is expected to realize polarity-free characteristics without any excessive antenna area. Minimum unit area is also smaller than the UMD antenna. It requires only one Schottky barrier diode in a unit. However, completely polarity-free antenna has not been reported. Therefore, we surveyed PFP design based on a patch Antenna for Circular Polarized Wave (ACPW).

Figure 13 shows the patterns we tested: (a) square, (b) rectangle (normal patch), (c) circle, (d) octagon, (e) chamfered a pair of opposing-corners of square by 45 degrees (ACPW), (f) chamfered a pair of opposing-corners of square circularly (Leaf type), (g) chamfered a pair of both end-corners of square circularly (Bathtub type) and (h) chamfered all corners of square circularly. Glass-epoxy (sanhayato Corp.) whose dielectric constant was about 4.5 was used as the insulating substrate. The size of patch in the resonance direction is λ/2.

The substrate was pre-coated with photosensitive paint and left the antenna-patterns coating by developing. Then the unnecessary cupper area was removed by substrate etching.

We measured the power conversion efficiency as a function of antenna angle ψ. Figure 14 shows some of them. As seen in the figure, the Leaf type showed the most flat angle dependency among all the antenna patterns, smoother than the ACPW type. Its power conversion efficiency is about 40% of the peak efficiency of the rectangle patch antenna.

Figure 15 shows the effect of its curvature radius on the conversion efficiency. The Leaf type with the curvature radius $r/(\lambda/2)=0.33$ showed the best polarity-free characteristics. Its conversion efficiency $P_{measured}/P_{rec\_max}$ varied only 33% to 40% for the 360 deg change of ψ.

Another important rectenna element is the rectifier. We adopted the microstrip-line circuits as shown in Fig. 16. Although the capacities of condensers, characteristics of Schottky barrier diodes and stub length would be the key parameters for efficient rectification, we tested two types of diodes, 1ss97 (NEC) and 1ss108 (HITACHI), and the effect of stab presence. A chip condenserGRM42-6 SL330J (muRata) is used as a bypass capacitance for output filter. The substrate material and the fabrication method of the rectifiers were the same as that of patch.

Table 2 shows that the measured rectification efficiency. Unfortunately, present efficiency is about 5% that is not enough to drive a motor for a MAV. However, we'll be able to improve it up to 50% by optimizing the parameters.

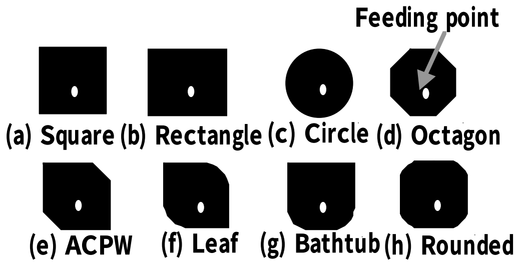

Figure 13. Antenna patterns. ACPW: Antenna for Circular Polarization Wave.

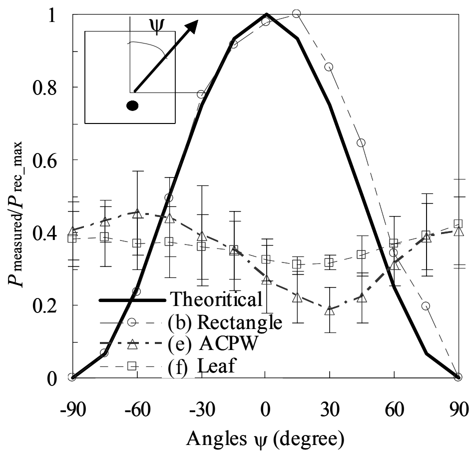

Figure 14. Relationship between angles and efficiencies.

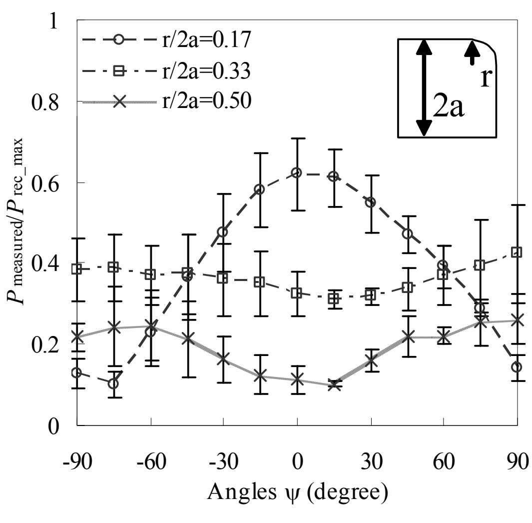

Figure 15. Effect of a round chamfering radius.

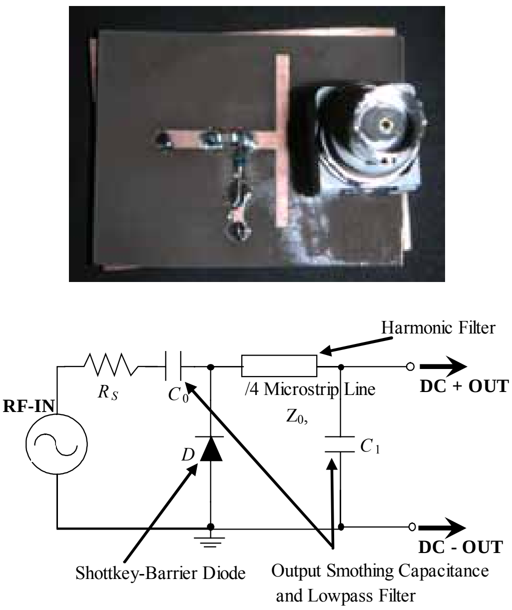

Figure 16. In-house rectifier.

Table 2. Measured Rectifiers' efficeincies

diode	stab length	efficiency (%)
1ss97 (NEC)	No stab	4.86
	7 mm	2.02E-6
1ss108 (HITACHI)	No stab	5.86E-1
	7 mm	1.33E-2

IV. Conclusion

We proposed the auto tracking system using a 2.45GHz microwave pilot signal and the software retro-directive function. Experimental simulation using an oscillator and a phase shifter in place of two antennas showed that the incident angle of the pilot signal could be uniquely determined by the simple microwave operation in our system.

A Polarity Free Patch antenna is proposed as a receiver antenna for constant power supply to a circling vehicle. The Leaf type patch with the curvature radius of $r/(\lambda/2)=0.33$ showed the best polarity-free characteristics among various patch shapes tested. Its conversion efficiency varied only in the range from 33% to 40% for the 360 deg change of ψ.

References

[1] Shinohara N. and Matsumoto H.: Experimental study of large rectenna array for microwave energy transmission, *IEEE Trans. on Microwave theory and Techniques*, 46 (3), pp. 261-268, 1998.

[2] Fusco V. F., Roy R., Karode S. L., "Reflector effects on the performance of a retrodirective antenna array," *IEEE Trans. on Antennas and Propagation*, Vol. 48, No. 6, 2000, pp. 946-953.

[3] Kaya N., Kojima H., Matsumoto H., et al.: ISY-METS Rocket Experiment for Microwave Energy Transmission, *ACTA Astronautica*, 34, pp. 43-46,1994.

[4] Komurasaki, K., Nakagawa, T., Ohmura, S., Arakawa, Y., "Energy Transmission in Space Using an Optical Phased Array," *Trans. JSASS, Space Technology Japan*, Vol. 3 (2005), pp.7-11

[5].R.J.Gutmann and J.M.Borrego, " Power Combining in an Array of Microwave Power Recitifiers " *IEEE-Trans. MTT*, Vol27, No.12,pp, 958-968,1979.

[6] Itoseisan, " Solar Power Satellite receipt site ball bureau terminal element " Rectenna " about basic research " Science research subsidy general research B result report,1982.